CHAPTER

11

Copper oxide as a corrosion inhibitor

Priyabrata Banerjee[1,2], *Sirsendu Sengupta*[1,2], *Manilal Murmu*[1,2] *and Naresh Chandra Murmu*[1,2]

[1]Surface Engineering and Tribology Group, CSIR-Central Mechanical Engineering Research Institute (CMERI), Durgapur, West Bengal, India [2]Academy of Scientific and Innovative Research (AcSIR), Ghaziabad, Uttar Pradesh, India

11.1 Introduction

Corrosion is defined as the deterioration or damage of metals and their alloys due to the harsh and corrosive nature of the environment. Corrosion adversely deteriorates or decreases the efficiency of equipment made of metallic materials. There are several consequences of the corrosion effects that affect mankind (Karpakam et al., 2011; Raja et al., 2016; Shaterian et al., 2015; Solmaz et al., 2011; Umoren & Eduok 2016). Every year, billions of steel materials are damaged due to corrosion (Huang et al., 2014; Ruhi et al., 2014). Therefore the protection of metal substrates from corrosion is important and the innovation of viable economical processes might prevent the losses of billions of dollars per annum. Metal and its alloys are used in several marine applications because of their cost-effectiveness. These metallic materials play a vital role in our life due to their widespread applications in the fields of automobiles, company machinery, domestic products, industry, and for domestic purposes (Sengupta, Murmu, Mandal, et al., 2021; Stipaničev et al., 2013; Zhu et al., 2017). Consequently, the effect of corrosion on metallic materials creates different concerning issues, such as loss of several resources, the collapse of existing facilities, environmental pollution, and so on (Dhineshbabu et al., 2016; Fiala et al., 2019; Soufeiani et al., 2020; Zhang et al., 2019). In recent times, the most economical, highly effective and well-organized technique for the inhibition of corrosion damage is the use of the corrosion-inhibiting materials as additives in the targeted solutions to which the metal substrates are exposed. Generally, corrosion inhibitors are utilized to diminish the rate of the corrosion reaction through several corrosion inhibition mechanism processes, such as minimizing the rate of cathodic or anodic corrosion current density, reducing the rate of diffusion toward the metal surfaces, and enhancement of electrical resistance or

Inorganic Anticorrosive Materials
DOI: https://doi.org/10.1016/B978-0-323-90410-0.00012-X

polarization resistance of the surfaces of the targeted metal by the creation of a passive oxide layer on the targeted metal surfaces or the formation of an insoluble complex (Arab & Noor 1993; Arenas et al., 2002; Bentiss et al., 2000; Chetouani & Hammouti 2003).

The corrosion-inhibiting materials may be of an organic or inorganic nature. Several inorganic corrosion inhibitors, such as chromates, phosphates, arsenates, etc., are the most used (Selvaraj et al., 2019). The use of metal oxides as anticorrosive materials is also quite popular. Currently, the unique properties of metal oxides from their corresponding bulk counterparts are receiving major attention. Furthermore, these metal oxides have a broad area of applications due to their enhanced physical as well as chemical behavior which is due to their small size, very high surface area, and tunable optical band gap (Gao et al., 2008; Gong et al., 2013).

Among other metal oxides, copper(II) oxide or cupric oxide, i.e., CuO, forms a monoclinic structure and behaves like a semiconductor in nature (especially p-type), consists of a very narrow bandgap, and also plays a vital role in protecting the metal substrate from its corrosive dissolution. Recently, after thorough investigation, nanostructured CuO has been synthesized and fabricated on copper surfaces. The CuO nanostructure possesses a large surface area, narrow bandgap (approx. 1.2 eV), and better physical and chemical properties. Hence, it finds diverse applications, such as anodes for batteries, sensors, catalyst, energetic materials, superconductors, and making hydrophobic surfaces (Dhineshbabu et al., 2016; Fiala et al., 2019; Soufeiani et al., 2020; Zhang et al., 2019). Furthermore, nanostructures of CuO exist in different morphological arrangements; nanoparticles, nanowires, nanorods, and nanotubes have been extensively reported (Liu et al., 2008; She et al., 2012). The CuO nanostructures are synthesized by thermal oxidation, chemical oxidation, electrodeposition, and hydrothermal processes. It is noteworthy to mention that the conversion of CuO nanostructures from $Cu(OH)_2$ nanostructures occurs without any changes of morphology and can be accomplished through dehydration by the heat treatment process. Generally, $Cu(OH)_2$ exists in a metastable phase, which is thermodynamically most stable and can be effortlessly converted to CuO during the pathway of gaining more stability (Cudennec & Lecerf 2003). Thereafter, the conversion happens in solid-state media at comparatively very low temperature by a thermal dehydration process and this conversion occurs in an aqueous environment at room temperature (Singh et al., 2009). The CuO is also used for anticorrosive applications in a harsh environment. Furthermore, CuO mixed with organic entity can enhance the anticorrosive performances because of the development of a thin film on the targeted metal surfaces (Kumar et al., 2020).

This chapter summarizes the use of copper oxide as a corrosion inhibitor in adverse corrosive conditions on various targeted metals. The adsorption capability of corrosion inhibitors on the surfaces of targeted metal depends upon several features, such as the distribution of the electron cloud throughout the structure of corrosion inhibitors, the nature of corrosive environments, the temperature of corrosive environments, the variety of targeted metals, as well as the surface charge of the metals. Furthermore, the synergistic increase of the anticorrosion property of CuO mixed with an organic entity, such as reduced graphene oxide, epoxy, etc., that is used for the protection of metallic materials in harsh corrosive conditions has been critically summarized.

11.2 Metallic deterioration and its protection from corrosive environment

The corrosion reaction of metals in the presence of corrosive conditions is a straightforward or a single-step reaction which occurs in the presence of oxygen. Furthermore, a corrosion reaction may proceed through a more complicated pathway or occur in two or more steps. For example, the reaction of iron with water or acidic conditions leads to corrosive dissolution. If two or more different types of metals come into contact with each other in the presence of saltwater like corrosive conditions or metals are under specific conditions, then the corrosion reactions proceed through complicated steps.

The plausible mechanism for the corrosion reaction of metals is through the electrochemical process. For simplicity, the mechanisms of the corrosion reaction of iron (Fe), aluminum (Al), and copper (Cu) in the neutral medium are briefly discussed here. It is reported that at the anode Fe^{2+} and Fe^{3+} ions are produced with a loss of electrons, while the reduction of oxygen takes place at the cathode, as shown in Eq. (11.1) and Eq. (11.2), respectively (Popova et al., 2003).

$$Fe \rightarrow Fe^{(2+/3+)} + 2e^- / 3e^- \tag{11.1}$$

$$O_2 + 2H_2O + 4e^- \rightarrow 4OH^- \tag{11.2}$$

The chloride ion (Cl^-) from the neutral solution acts as a nucleophile, which attacks the iron's surface atoms and forms a complex, iron chloride, $FeCl_3$. Furthermore, the $FeCl_3$ reacts with water to form more stable iron hydroxides, i.e, $Fe(OH)_2$ and $Fe(OH)_3$. In addition, hydrochloric acid is formed.

$$Fe + 2Cl^- \rightarrow FeCl_2 \tag{11.3}$$

$$Fe + 3Cl^- \rightarrow FeCl_3 \tag{11.4}$$

$$FeCl_2 + 2H_2O \rightarrow Fe(OH)_2 + 2HCl \tag{11.5}$$

$$FeCl_3 + H_2O \rightarrow Fe(OH)_3 + 3HCl \tag{11.6}$$

In the absence of a chloride environment, it reacts with another nucleophile, i.e., a hydroxide ion (OH^-) to form iron hydroxide as a product (Popova et al., 2003).

$$Fe^{2+} + 2OH^- \rightarrow Fe(OH)_2 \tag{11.7}$$

$$Fe^{2+} + 3OH^- \rightarrow Fe(OH)_3 \tag{11.8}$$

Thus the presence of chloride ions in aqueous medium results in an enhancement of the rate of the iron corrosion reaction through the formation of intermediate species and corrosive hydrochloric acid.

Aluminum has corrosion resistance capabilities by the formation of oxide layer on its surface (Xhanari & Finšgar, 2019). However, Al shows corrosion when it is exposed to a chloride environment due to the degradation of the protective layer. The reactions at the anode are as follows:

$$Al \rightarrow Al^{3+} + 3e^- \tag{11.9}$$

$$AlCl_3 + 3H_2O \rightarrow Al(OH)_3 + 3HCl \tag{11.10}$$

From Eq. (11.10), it is revealed that at the anode the environment becomes more acidic and it causes the Al to undergo electrodissolution. The reactions taking place at the cathode are shown as follows:

$$AlCl_3 + 3H_2O \rightarrow Al(OH)_3 + 3HCl \tag{11.11}$$

$$3H^+ + 3e^- \rightarrow \frac{3}{2}H_2 \tag{11.12}$$

$$AlCl_3 + 3H_2O \rightarrow Al(OH)_3 + 3HCl \tag{11.13}$$

Hence, due to the occurrence of such chemical reactions, the pitting corrosion on Al surfaces takes place.

Copper is one of the most significant nonferrous metals which possesses high longevity in a neutral medium (pH = 7), such as in water distribution networks, etc. Titze and Strehblow revealed that a passive layer of copper oxide exists as a duplex structure of its oxide: cuprous oxide is present in the inner sphere and cupric hydroxide is present in the outer-sphere (Strehblow & Titze 1980). Generally, the copper does not take part in a corrosion reaction in nonoxidizing acidic conditions, because the evolution of hydrogen is not participating through its corrosion method. However, if the involvement of oxygen or some other oxidant species such as Fe^{3+}, NO_3^-, and SO_4^{2-} ions are present then the corrosion reaction becomes vital. The stability of copper oxide is higher in a basic medium or at very high pH (pH = 8–12) (Brusic et al., 1991), but at low pH or in an acidic medium its surface starts to become rough.

$$Cu_2O + 2H^+ \rightarrow 2Cu^+ + H_2O \tag{11.14}$$

$$CuO + 2H^+ \rightarrow Cu^+ + H_2O \tag{11.15}$$

Additionally, cuprous (Cu^+) ions may participate in a disproportionation reaction, as shown in Eq. (11.16).

$$2Cu^+ \rightarrow Cu^{2+} + Cu \tag{11.16}$$

The uncontaminated copper at pH = 7 as well as in a moderately alkaline medium exhibits, three anodic peaks due to the production of Cu_2O, CuO and $Cu(OH)_2$, as revealed from potentiodynamic study. At first, Cu_2O is produced, which consequently oxidizes to CuO. Also, at additional positive potentials it may be converted to $Cu(OH)_2$ (Metikoš-Huković, Babić, & Marinović, 1998).

$$2Cu + H_2O \rightarrow Cu_2O + 2H^+ + 2e^- \tag{11.17}$$

$$Cu_2O + H_2O \rightarrow CuO + 2H^+ + 2e^- \tag{11.18}$$

$$Cu_2O + 3H_2O \rightarrow Cu(OH)_2 + 2H^+ + 2e^- \tag{11.19}$$

It has been known that several effective corrosion inhibitors are used to prevent unwanted corrosion reaction on copper and its alloy. Furthermore, under atmospheric and immersed situations, the discoloration of the copper surface is minimized by the addition of inhibitor molecules, since it forms a protective film on copper surfaces.

11.3 Copper oxide as corrosion inhibitor

Chromate, molybdate, nitrite and orthophosphate are the most frequently used inorganic corrosion inhibitors, although these inhibitor molecules have a few limitations, including high cost, poor biodegradability and toxic nature. Furthermore, it is observed that pitting corrosion occurs at the surface. Thus, the main challenge in scientific communities is to develop some inorganic anticorrosive materials which are eco-friendly and less toxic (Selvaraj et al., 2019).

Selvaraj et al. reported that copper oxide (CuO) nanoparticles incorporated during the polymerization of aniline form a copper oxide–polyaniline composite, CuO-PANI, which has been used as an anticorrosive material on targeted mild steel in an acidic medium (Selvaraj et al., 2019). Initially, the characterization of CuO, polyaniline, and CuO-PANI was performed by Fourier-transition infrared spectroscopy, which confirmed its desired formation (Fig. 11.1).

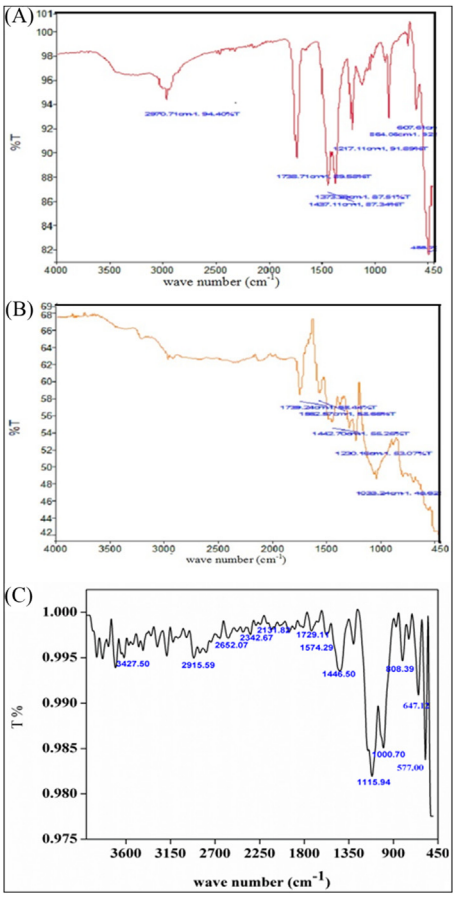

FIGURE 11.1 Fourier transition infrared spectrum of (A) copper oxide, (B) polyaniline, and (C) copper oxide-polyaniline composite. Source: *From Selvaraj, P.K., Sivakumar, S., & Selvaraj, S. (2019). Embargo nature of CuO-PANI composite against corrosion of mild steel in low pH medium.* Journal of Electrochemical Science and Technology, *10(2), 139–147. https://doi.org/10.5229/JECST.2019.10.2.139*.

Conducting polymers are superhydrophobic in nature, which is why it plays an important role in corrosion inhibition by inhibiting the ingress of dissolved corrosive ingredients in the corrosive solution to penetrate the metal substrates. Moreover, after the addition of CuO nanoparticles, the hydrophobicity of the above polymer is enhanced, and consequently its corrosion protection efficacy in adverse corrosive conditions is increased. The surface morphology revealing its corrosion inhibiting property has been explored using scanning electron microscopes of pure CuO and CuO-PANI composites, as given in Fig. 11.2.

The efficiency of the synthesized anticorrosive material has been explained via potentiodynamic polarization (PDP) and electrochemical impedance spectroscopy (EIS) methods. PDP curves or Tafel plots, as shown in Fig. 11.3, reveal that the corrosion current density was decreased steadily with an increase in the addition of the synthesized composite materials. The potentiodynamic parameters of the targeted metal sample in the test solution are depicted in Table 11.1. The decrease in the corrosion current density suggests an effective increase in the corrosion inhibition capability.

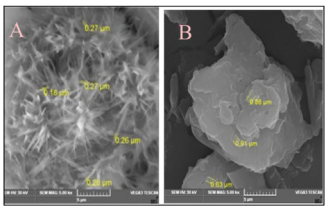

FIGURE 11.2 Scanning electron microscopes images of (A) copper oxide, and (B) copper oxide- polyaniline composite. Source: *From Selvaraj, P.K., Sivakumar, S., & Selvaraj, S. (2019). Embargo nature of CuO-PANI composite against corrosion of mild steel in low pH medium.* Journal of Electrochemical Science and Technology, *10(2), 139–147. https://doi.org/10.5229/JECST.2019.10.2.139.*

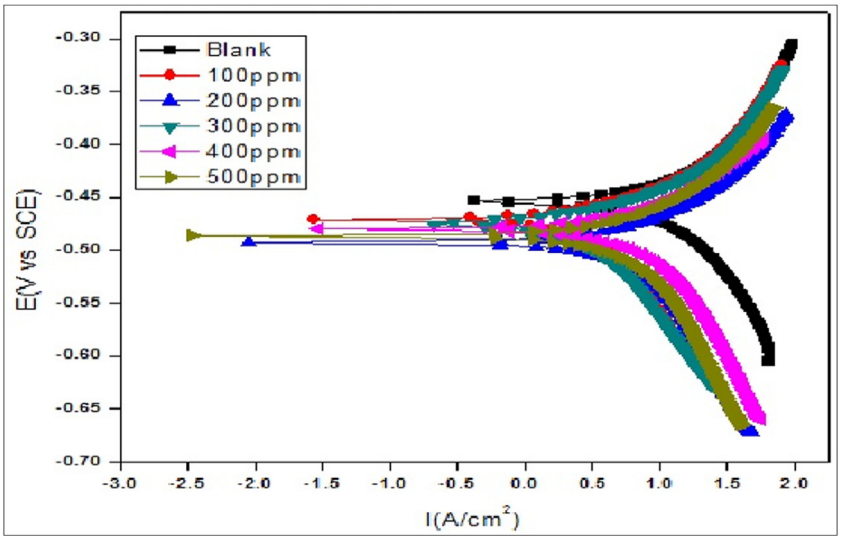

FIGURE 11.3 Potentiodynamic polarization curves for mild steel in blank and with the addition of inhibitor added test solution. Source: *From Selvaraj, P.K., Sivakumar, S., & Selvaraj, S. (2019). Embargo nature of CuO-PANI composite against corrosion of mild steel in low pH medium. (20C.E.).* Journal of Electrochemical Science and Technology, *10(2). https://doi.org/10.5229/JECST.2019.10.2.139.*

The EIS results suggest the enhancement of the size of the capacitive loop with the addition of synthesized inhibitors, because the adsorption of inhibitors on targeted metal surfaces and the formation of a thin layer on metal surfaces can shield the movement of the corrosion current toward the metallic surfaces and behave as excellent inhibition performances in a very low pH corrosive environment. Furthermore, the development of shielding film at the electrolyte/metal interface causes the increase of charge transfer resistance (R_{ct}) values and increasing the electrical double layer thickness causes the decrease in the double-layer capacitance (C_{dl}) values (Fig. 11.4). From the tabulated data in Table 11.2, it is clear that CuO-PANI composite acts as an efficient inhibitor on targeted metal surfaces in low pH environments.

TABLE 11.1 Potentiodynamic polarization parameters obtained for mild steel in blank and with the addition of inhibitor added test solution.

Conc. of composite (ppm)	$-E_{corr}$ (mV vs SCE)	b_a (mVdec^{-1})	b_c (mVdec^{-1})	i_{corr} (μA cm^{-2})	Inhibition efficiency	Surface coverage(θ)
Blank	455	61	63	1960	–	–
100	478	55	63	837	57	0.5729
200	491	42	55	603	69	0.6923
300	476	84	47	507	74	0.7413
400	480	14	15	494	75	0.7479
500	511	22	26	325	83	0.8341

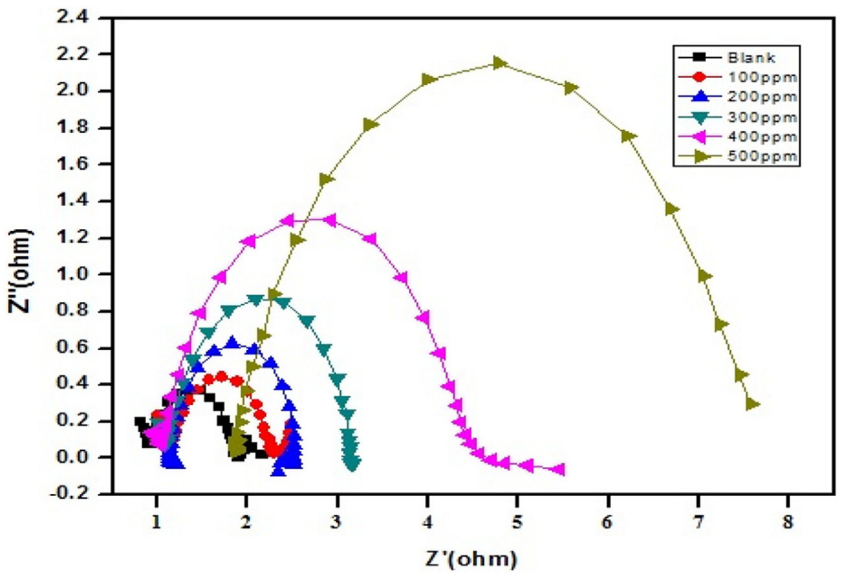

FIGURE 11.4 Nyquist impedance diagrams for mild steel in 1 M blank and with the addition of test solution.

TABLE 11.2 EIS parameters obtained for mild steel in 1 M blank and with the addition of test solution.

Conc. of composite (ppm)	R_s (Ω)	C_{dl} (μF cm^{-2})	R_{ct} (Ω cm^2)	Inhibition efficiency (%)	Surface coverage (θ)
Blank	1.154	553	1.275	–	–
100	1.167	438	1.362	06	0.0630
200	1.097	437	2.043	38	0.3795
300	1.128	633	3.941	68	0.6764
400	1.022	535	4.169	69	0.6941
500	2.052	439	5.934	78	0.7851

From Selvaraj, P.K., Sivakumar, S., & Selvaraj, S. (2019). Embargo nature of CuO-PANI composite against corrosion of mild steel in low pH medium. Journal of Electrochemical Science and Technology, *10(2), 139–147. https://doi.org/10.5229/JECST.2019.10.2.139.*

Xiao et al. reported a superhydrophobic CuO nanoneedle (NNA) used as an anticorrosive agent on copper surfaces in the presence of harsh corrosive conditions (Xiao et al., 2015). The anticorrosion performance of CuO-NNA film was evaluated with the help of EIS and PDP techniques. The corrosion inhibition efficiency $\eta(\%)$ of CuO-NNA film on the copper surface is calculated using the following equation:

$$\eta(\%) = \frac{j_0 - j_{\text{corr}}}{j_0} \tag{11.20}$$

where j_o and j_{corr} refer to corrosion current density of pristine copper coupon and modified copper coupon, respectively. The change in static contact angle plays an important role in the determination of the stability of superhydrophobic CuO-NNA surfaces in the presence of pure water and 1.5 wt.% and 3.5 wt.% aqueous NaCl environments. Furthermore, CuO-NNA modified by fluoroalkylsilane (FAS-17) and then the anticorrosive behavior of the synthesized composite in the presence of the 3.5 wt.% NaCl environment was calculated using electrochemical techniques which also revealed its high corrosion inhibition property.

The schematic diagram of CuO-NNA film on the surface of copper is shown in Fig. 11.5.

The corrosion protection mechanism by superhydrophobic CuO-NNA film has been presented in Fig. 11.5. Additionally, Fig. 11.6 shows a schematic model that can demonstrate the solid–liquid interfaces between the CuO-NNA and corrosive NaCl solutions. CuO-NNA molecules can be adsorbed on Cu surfaces to form a thin protective layer and protect the metal from corrosion.

Furthermore, the capability to improve the corrosion inhibition performance in a marine environment by the addition of TiO_2 and CuO nanocomposites as nanofillers for the epoxy coating to prevent the targeted metal surfaces from corrosion has been recently reported by (Kumar et al., 2020). The effect of corrosion inhibitory performances was calculated after the addition of TiO_2 and CuO nanocomposites into the epoxy and utilized as a coating material on the mild steel surfaces using the EIS technique in 3.5% NaCl environments. The corresponding EIS results are shown in Fig. 11.7. The synthesized epoxy coating materials in the absence and presence of 5%, 10%, and 20% TiO_2-CuO nanocomposite were

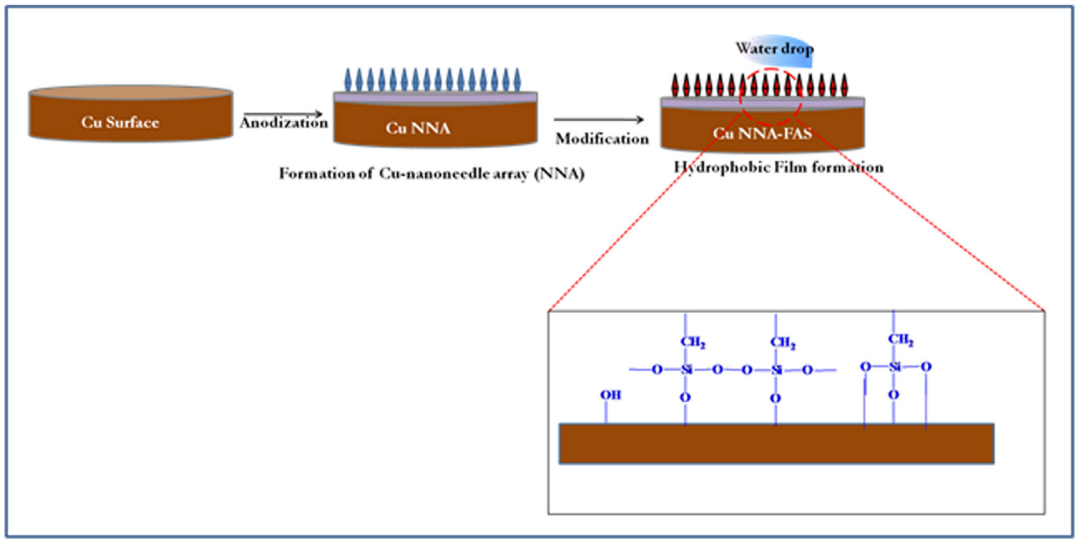

FIGURE 11.5 Schematic diagram of CuO-NNA stepwise fabrication methods: (A) CuO-NNA film growing on Cu surfaces via anodization method; (B) creation of superhydrophobic Cu surfaces by the fluorosilanization of CuO-NNA film.

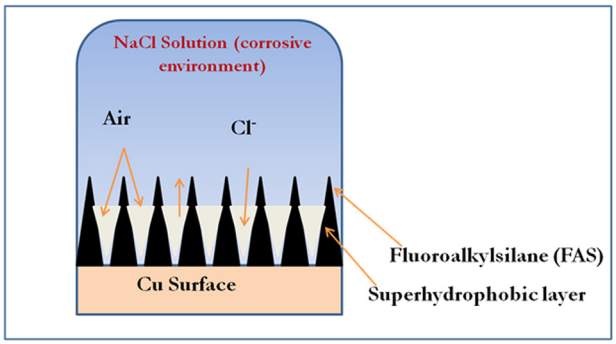

FIGURE 11.6 Schematic representations of the CuO-NNA superhydrophobic surface in a 3.5 wt.% NaCl environment.

represented as PE, PE5CTN, PE10CTN, and PE20CTN, respectively. After the addition of the nanocomposite on the epoxy coating materials, the transparency of the system is reduced, but if the concentration of the nanocomposite is increased then the color of the epoxy coating turns to light brown. The EIS results were examined using an equivalent circuit fitting in order to get a suitable behavior of coating materials on the metal sample in harsh corrosive conditions. Thereafter, several electrochemical parameters such as solution resistance (R_s), charge transfer resistance (R_{ct}), film resistance (R_f), double-layer capacitance (Q_{dl}), and film capacitance (Q_f) were determined with the help of EIS data. The electron transfer occurs between the metal/coating interfaces region. In general, electron transfer of the synthesized molecules toward the metal surfaces can be measured by the R_{ct} value. High R_{ct} values signify the minimized rate of corrosion of the targeted metal,

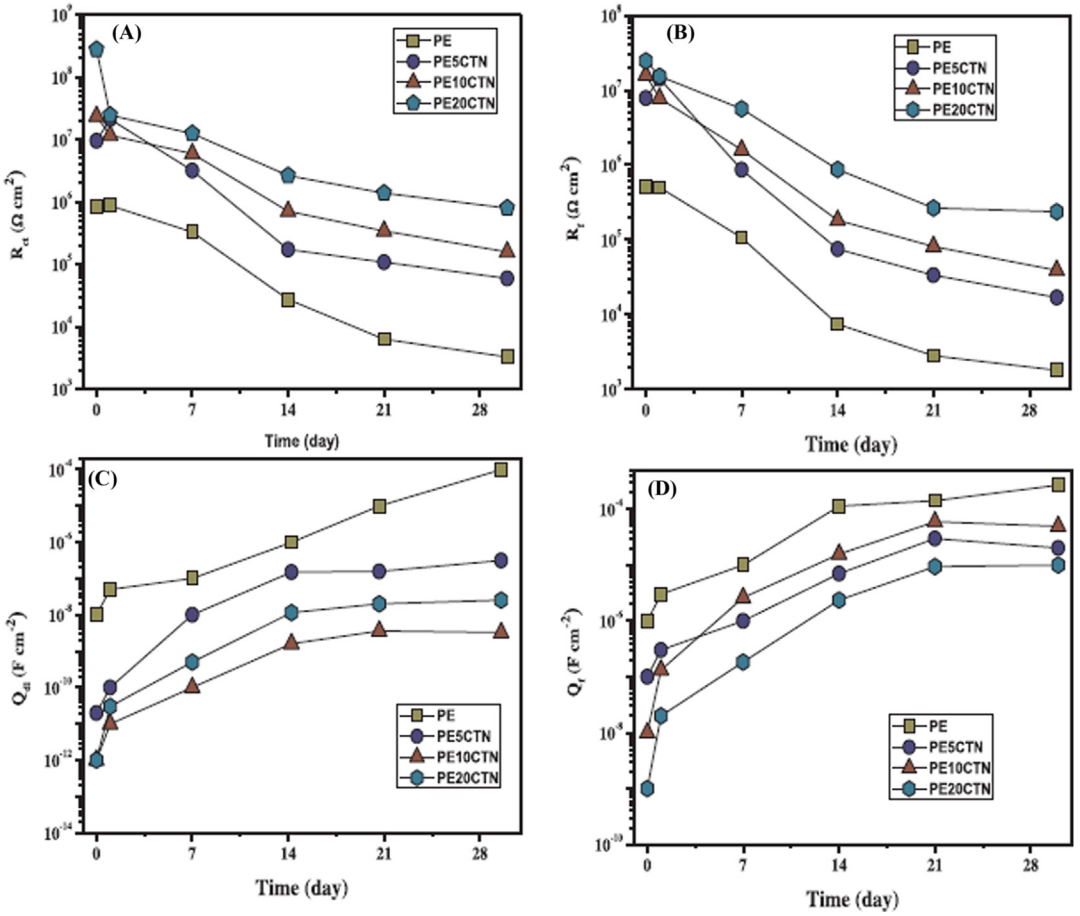

FIGURE 11.7 EIS parameters (A) charge transfer resistance, (B) film resistance, (C) double-layer capacitance, and (D) film capacitance for coated mild steel surfaces after immersion for 30 days in a 3.5% NaCl environment. *EIS*, Electrochemical impedance spectroscopy. Source: *Kumar, A. M., Khan, A., Suleiman, R., Qamar, M., Saravanan, S., & Dafalla, H. (2018). Bifunctional CuO/TiO_2 nanocomposite as nanofiller for improved corrosion resistance and antibacterial protection.* Progress in Organic Coatings, *114*, 9–18. https://doi.org/10.1016/j.porgcoat.2017.09.013.

implying it possesses excellent protection ability of the synthesized molecules against corrosive conditions (Sengupta, Murmu, Murmu, et al., 2021; Stipaničev et al., 2013; Zhu et al., 2017). Furthermore, in the case of a pure epoxy coating, the charge transfer resistance value decreases, which indicates a retardation of the corrosion or redox reactions on mild steel samples during the immersion periods. However, R_{ct} values revealed that the inclusion of CuO-TiO_2 nanocomposite has a better protection ability than an epoxy coating. It implies that the anticorrosive efficacy of the CuO-TiO_2 nanocomposite is greater compared to the epoxy coating on mild steel surface immersed in 3.5% NaCl solution. Furthermore, in the case of epoxy nanocomposite (CuO-TiO_2) coatings, pits and holes have been filled or minimized by the nanoparticles of the synthesized metal oxide and

enhance the protection efficiency (PE) of the coating materials which can be explained by the smaller Q_{dl} value than that of the pure epoxy coating materials at the same exposure time (Ma et al., 2003; Martini & Muller 2000). Electrochemical studies play an important or key role in the determination of the anticorrosion efficiency of CuO-TiO_2 nanocomposites with epoxy coating materials on mild steel surfaces in the presence of 3.5% NaCl environments.

In another investigation, the composite of polycaprolactone (PCL) with zinc oxide (ZnO), nickel oxide (NiO), copper oxide (CuO) separately as polycaprolactone/zinc oxide (PCL/ZnO), polycaprolactone/nickel oxide (PCL/NiO), polycaprolactone/copper oxide (PCL/CuO), and mixed form as polycaprolactone/zinc oxide−nickel oxide−copper oxide (PCL/ZnO-NiO-CuO) have been effectively fabricated and deposited on targeted mild steel surfaces with the help of electrospinning techniques. Subsequently, the corrosion inhibition efficiency was determined using electrochemical methods, such as open circuit potential (OCP), EIS, and PDP in the presence of a 1 M HCl solution (AlFalah et al., 2020). The main aim of this investigation was to calculate the effect of coating, especially electrospun composite nanofiber coatings on targeted metal surfaces and also to inhibit the metallic corrosion in a 1 M HCl solution. The FT-IR data confirmed the allocation of ZnO, NiO, and CuO into the PCL matrix, as shown in Fig. 11.8.

Furthermore, OCP versus time curves (Fig. 11.9) for mild steel samples with the addition of synthesized anticorrosive materials, such as coated with PCL/ZnO, PCL/NiO, PCL/CuO, and PCL/ZnO-NiO-CuO on the targeted metal samples in 1 M HCl medium, reflect the negative potential value with increasing time. Subsequently, some positive potential value is shifted until it attains a steady state. OCP plays a key role, such that a positive shift of OCP signifies the passive conditions of underlying metal due to the development of a thin layer on the targeted metal surfaces, as well as exhibiting excellent anticorrosion performances. Thereafter, a more positive value of OCP gives significant information about the CuO/PCL composite used as an anticorrosive agent in the presence of destructive ions like hydrogen and chloride ions on targeted mild steel surfaces.

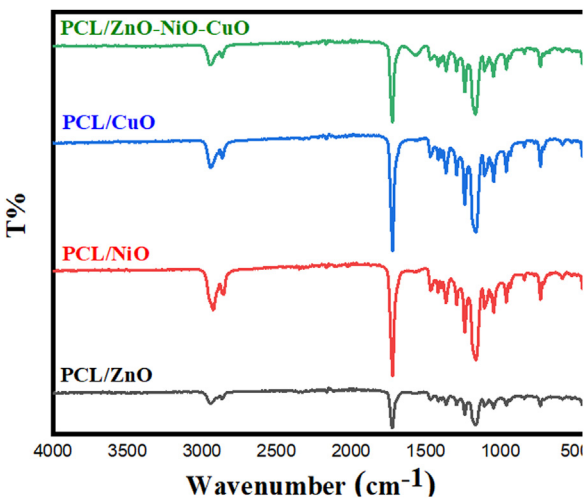

FIGURE 11.8 FT-IR spectra of PCL/ZnO, PCL/NiO, PCL/CuO, and PCL/ZnO-CuO-NiO nanofiber film. Source: *From AlFalah, M. G. K., Kamberli, E., Abbar, A. H., Kandemirli, F., & Saracoglu, M. (2020). Corrosion performance of electrospinning nanofiber ZnO-NiO-CuO/polycaprolactone coated on mild steel in acid solution.* Surfaces and Interfaces, *21, 100760. https://doi.org/10.1016/j.surfin.2020.100760.*

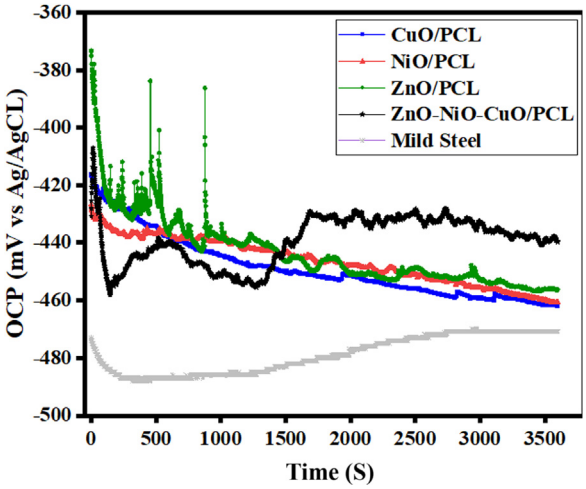

FIGURE 11.9 Open circuit potential for bare and coated mild steel with nanofiber film in 1 mol L^{-1} HCl solution. Source: *From AlFalah, M. G.K., Kamberli, E., Abbar, A.H., Kandemirli, F., & Saracoglu, M. (2020). Corrosion performance of electrospinning nanofiber ZnO-NiO-CuO/polycaprolactone coated on mild steel in acid solution.* Surfaces and Interfaces, *21, 100760. https://doi.org/10.1016/j.surfin.2020.100760.*

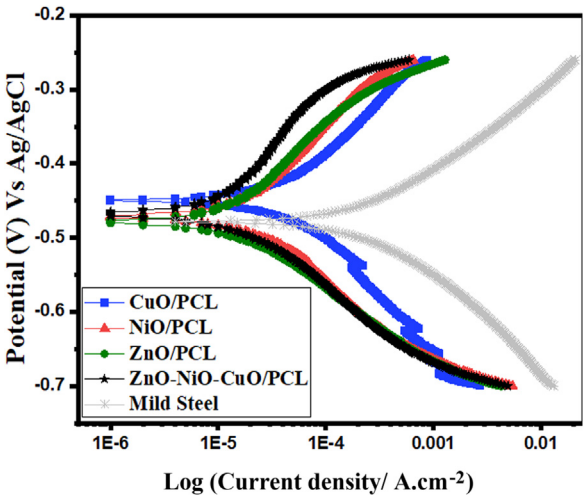

FIGURE 11.10 Potentiodynamic polarization curves for bare and coated mild steel with nanofiber film in 1 mol L^{-1} HCl solution. Source: *AlFalah, M.G.K., Kamberli, E., Abbar, A.H., Kandemirli, F., & Saracoglu, M. (2020). Corrosion performance of electrospinning nanofiber ZnO-NiO-CuO/polycaprolactone coated on mild steel in acid solution.* Surfaces and Interfaces, *21, 100760. https://doi.org/10.1016/j.surfin.2020.100760.*

PDP results show the shifting of Tafel plots, resulting in a decrease of corrosion current density, as shown in Fig. 11.10 for all the coating materials. It suggests that the applied coating strongly inhibits the corrosive dissolution of the metals immersed in a corrosive solution. Moreover, in Fig. 11.10 it is observed that both cathodic and anodic curves were shifted toward the lower current density, which confirms the existence of coating materials on the mild steel surfaces. The applied inhibitor creates a thin film on mild steel surfaces, thereby retarding the movement of corrosive ions and the ongoing corrosion reactions. The Nyquist plot, as shown in Fig. 11.11, revealed that the applied coating exhibits high corrosion inhibition, as reflected in the high semicircle. It contains more roughness as well as inhomogeneity of the surfaces, although the inductive loop occurs at a low-frequency region because of

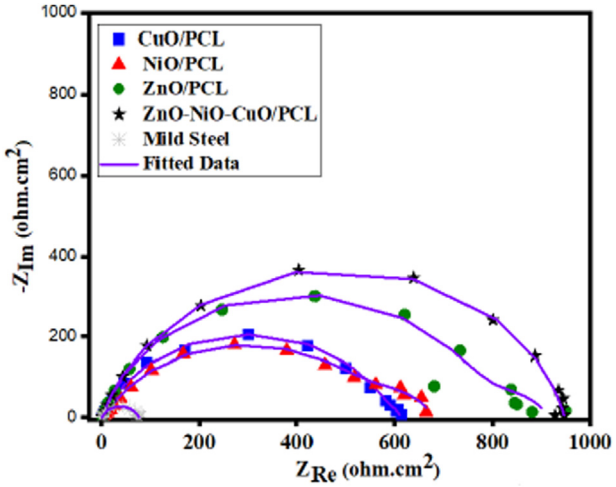

FIGURE 11.11 Nyquist diagram for blank and coated mild steel with nanofiber film in 1 mol L^{-1} HCl solution. *From AlFalah, M.G.K., Kamberli, E., Abbar, A.H., Kandemirli, F., & Saracoglu, M. (2020). Corrosion performance of electrospinning nanofiber ZnO-NiO-CuO/polycaprolactone coated on mild steel in acid solution.* Surfaces and Interfaces, *21, 100760. https://doi.org/10.1016/j.surfin.2020.100760.*

the adsorption of an intermediate species on the metal surfaces. The protection efficiency (PE (%)) was calculated using the relations:

$$PE(\%) = \frac{R_p - R_p^0}{R_p} \tag{11.21}$$

where R_p and R_p^0 are the coated and uncoated polarization resistance, respectively. The polarization resistance value of coated mild steel sample is larger than for the uncoated sample. Furthermore, after the application of the coating, the value increases and consequently the PE value is also increased.

The anticorrosion efficacy of electrospun ZnO-NiO-CuO/PCL composites on mild steel samples in the presence of 1 M HCl solutions can be explained by OCP, PDP, and EIS techniques. Owing to the development of a thin layer on the targeted metal surfaces, it repels all the corrosive species coming toward it. Secondly, the micro- and nanostructured CuO particles are used as composite additives for corrosion resistance on a mild steel sample (Deepa & Nayaka 2020). CuO is also used as an additive for a Zn-composite coating on targeted mild steel surfaces for corrosion inhibition.

Nowadays, researchers have synthesized several oxides of metal such as NiO, Al_2O_3, ZrO_2, and SiO_2, and used them as composite additives for Zn-coating (Adriana et al., 2010; Behzadnasab et al., 2011; Francesco et al., 2011; Mohammad et al., 2017). The sizes of the macro- and nanoparticles of the synthesized metal oxides play important roles for composite additives, because the corrosion protection of metal increases with the increase in the size of the particles. The accessibility of several metal oxides and their easy synthesis procedure is the main reason for using them as fabricating agents for composite coating (Lekka et al., 2009; Zanella et al., 2009). The CuO micro- and nanoparticle synthesis via a coprecipitation technique is a significant method due to its simple, low-cost synthesis that requires relatively less equipment. The synthesized CuO particles were used for Zn-micro as well as Zn-nano CuO composite coatings on targeted mild steel surfaces. The effect of

the size of the particles which are already used as composite material was observed and their corrosion protection abilities were also checked against the corrosive environment. After that, composite-coated metal samples were analyzed for corrosion detection purposes in 3.5% NaCl environments. The corrosion behavior of synthesized materials was analyzed by several electrochemical techniques, such as Tafel, EIS, etc. The crystalline sizes of CuO macro- and nanoparticles were determined with the help of X-ray diffraction spectra documented from an X-ray diffractometer. CuO particles exist in a spherical shaped flake-like morphology. Furthermore, it is clearly visible that when CuO particles are in the nanorange then the morphology is changed and they are converted to the spherical shaped nodular structure.

The morphology of bare Zn-coated samples exhibits an irregularly shaped surface arrangement and the grains are arranged haphazardly. The abnormality of the surface morphology was relatively enhanced for the Zn-micro-CuO composite coating than for the Zn-coating samples. Furthermore, the Zn-nano-CuO composite coating revealed a change in the morphology of the samples and it became more finely grained and had more uniformly arranged crystal structures. Therefore the investigation confirmed that the CuO nanoparticles are highly efficient for the homogeneity of the surfaces of the synthesized Zn-composite coating, in contrast to the CuO macroparticles coating.

The corrosion inhibition efficiency of Zn coating (Z_0), Zn-micro-CuO composite coating (Z_{II}), and Zn-nano-CuO composite coating ($^*Z_{II}$) on targeted metal surfaces was measured using the Tafel polarization method in a 3.5 wt.% NaCl environment. Tafel curves of the coating of Zn-micro-CuO composite with different concentrations of CuO microparticles are depicted as Z_I, Z_{II}, and Z_{III}. In the same way, Zn-nanocomposite coatings, such as $^*Z_I$, $^*Z_{II}$, and $^*Z_{III}$, were also presented in another Tafel plot.

The pure Zn-coated mild steel samples (Z_0) displayed very high negative E_{corr} as well as high i_{corr} values, which clearly signified that under harsh corrosive conditions the Zn-coating becomes more reactive than others. Furthermore, the E_{corr} value is shifted towards the more negative side and the i_{corr} value is maximum in case of metal coating of Zn-micro CuO composite which are depicted as Z_I, Z_{II}, and Z_{III} than a metal coating of Zn-nano CuO composite which are depicted as $^*Z_I$, $^*Z_{II}$, and $^*Z_{III}$. The lower value of i_{corr} reveals minimal chemical reactivity under corrosive conditions. The CuO nanoparticles efficiently blocked the active sites of the surface of targeted mild steel samples and protected it from corrosion.

The Nyquist plots of the Zn coating (Z_0), Zn-micro-CuO composite coating (Z_{II}), and Zn-nano-CuO composite coating ($^*Z_{II}$) were studied in 3.5 wt.% NaCl solution. It revealed that the Zn-nano CuO composite-coated materials exhibit a very high R_p value compared with the Zn-micro-CuO composite-coated materials. Among Zn-micro-CuO composite coatings (Z_I, Z_{II}, and Z_{III}), excellent corrosion inhibition properties were observed for Z_{II}. Among Zn-nano CuO composite coatings ($^*Z_I$, $^*Z_{II}$, and $^*Z_{III}$), and the $^*Z_{II}$ exhibited better anticorrosion behavior. The $^*Z_{III}$ exhibited lower corrosion inhibition efficacy than $^*Z_{II}$, since at higher concentrations, the particles become aggregated in the bath solution, resulting in bad inclusions of CuO in the Zn-matrix. Therefore the addition of CuO nanoparticles in the Zn matrix remarkably increases the anticorrosion efficacy in the presence of harsh or corrosive environments; and CuO nanoparticles act as an excellent corrosion inhibitor.

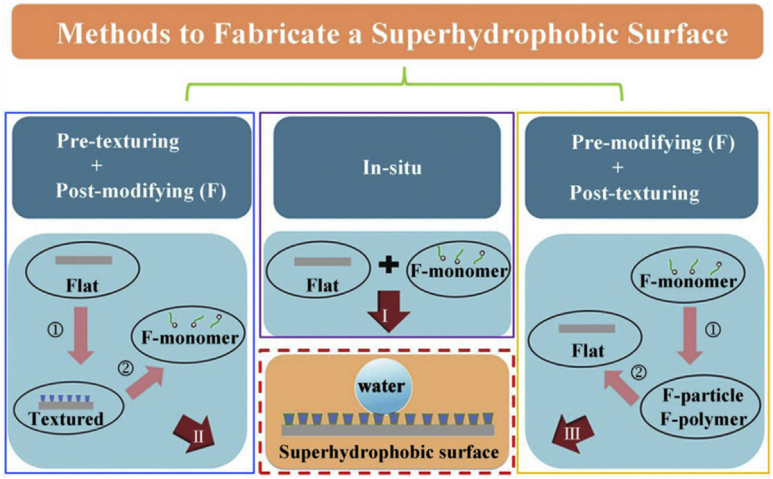

FIGURE 11.12 Schematic of methods used to develop a superhydrophobic coating material. Source:*From Yao, W., Liang, W., Huang, G., Jiang, B., Atrens, A., & Pan, F. (2020). Superhydrophobic coatings for corrosion protection of magnesium alloys.* Journal of Materials Science & Technology, *52, 100–118. https://doi.org/10.1016/j.jmst.2020.02.055*.

Similarly, another group of researchers also synthesized CuO particles and used them as additives for corrosion resistance on magnesium alloy in 3.5 wt.% NaCl solution (Yao et al., 2020). The CuO particles help in the development of superhydrophobic coating surfaces. The presence of several microstructures of copper dioxide plays a key role acting as a superhydrophobic coating, hence it is preferred for use as a corrosion inhibitor (Fan & Li 2011). She et al. (2012) built up superhydrophobic CuO coating materials through electroless Ni, electrodeposition of Cu-Zn, and electrochemical fabrication of CuO without any help from sophisticated instruments or any expensive reagents (She et al., 2012). Furthermore, it has been established that the superhydrophobic layer is formed on the metal substrates. It has been revealed that these coated materials showed better anti-corrosion performance than the bare substrate in a 3.5 wt.% NaCl environment over 1080 min exposure. The uncoated materials were comparatively more damaged in comparison to the coated materails which were exposed to corrosive solution for 1440 min immersion. The schematic diagram demonstrating the formation of the superhydrophobic coating is depicted in Fig. 11.12.

11.4 Summary and future perspective

Corrosion of metals and alloys is a worldwide concern in diverse fields, such as manufacturing, marine, oil refineries, and so on. The maintenance of metals and alloys to protect them from corrosion leads to a huge financial drain. The shielding of metals and alloys is therefore of paramount significance. The goal of studying the corrosion process is to reveal the most viable strategy to inhibit the corrosion process and provide shielding of the metallic substrates. The application of corrosion inhibitors is one of the important

approaches to prevent or mitigate the corrosion reaction. The mechanism of how corrosion inhibitors work is usually not known. It is, however, in general, accepted that, in most cases, the corrosion protection process proceeds via an interaction between the synthesized inhibitors and targeted metal surfaces, which results in the development of a thin protective layer on the targeted metal surfaces. In most cases, the empirical test has provided the effectiveness of the inhibitor molecules for a particular substrate in a particularly corrosive environment. Knowledge of surface chemistry acts as a key feature for describing the mechanism of corrosion inhibitors' action on a metal's surface in corrosive environments. Several surface analytical techniques are required for the determination of inhibitory action toward the metal surfaces. This chapter summarizes the use of copper oxide as an inorganic corrosion-inhibiting material for the protection of copper, iron, zinc, aluminum, and their alloys from corrosive environments and to minimize their degradation. The adsorption of the protective copper oxide layer on the metallic substrates has been found to act as a barrier that isolates it from the aggressive ingredients present in the corrosive environments under investigation. Furthermore, copper oxide has been incorporated as an inorganic anticorrosive additive in several organic coatings to enhance the corrosion inhibition property of the developed inorganic–organic composite coating. The adsorption capability of inorganic corrosion inhibitors on the metal surfaces is related to several factors, including their structure, electron cloud distribution, the type of corrosive environment, the temperature of the solution, the type of metal, the surface charge of the metal, and so on. The introduction of copper oxide with such an efficient inorganic corrosion inhibitor synergistically increases the corrosion inhibition. The development of copper oxide nanoparticle-based anticorrosive coating will be of broad research interest in the near future.

Acknowledgments

P.B. is very thankful to the Department of Higher Education, Science & Technology and Biotechnology, Govt. West Bengal, India for providing financial assistance to accomplish this research work [*vide* sanction order no. 78 (Sanc.)/ST/P/S&T/6G-1/2018 dated 31.01.2019 and project no. GAP-225612]. S.S. acknowledges the DST Inspire Fellowship, Department of Science and Technology, Govt. of India, New Delhi [IF180291]. MM acknowledges the National Fellowship for Higher Education of Schedule Tribes Students [formerly known as Rajiv Gandhi National Fellowship of Schedule Tribes Students] award letter no. F1-17.1/2014-15/RGNF-2014-15-ST-JHA-71559 granted by University Grants Commission and Ministry of Tribal Affairs, Govt. of India, New Delhi, India

References

Adriana, V., Simona, V., Aurel, P., Caius, B., & Liana, M. M. (2010). Electrodeposited Zn–TiO_2 nanocomposite coatings and their corrosion behavior. *Journal of Applied Electrochemistry*, *40*, 1519–1527. Available from https://doi.org/10.1007/s10800-010-0130-x.

AlFalah, M. G. K., Kamberli, E., Abbar, A. H., Kandemirli, F., & Saracoglu, M. (2020). Corrosion performance of electrospinning nanofiber ZnO-NiO-CuO/polycaprolactone coated on mild steel in acid solution. *Surfaces and Interfaces*, *21*, 100760. Available from https://doi.org/10.1016/j.surfin.2020.100760.

Arab, S. T., & Noor, E. A. (1993). Inhibition of acid corrosion of steel by some S-alkylisothiouronium iodides. *Corrosion*, *49*(2), 122–129. Available from https://doi.org/10.5006/1.3299206.

Arenas, M. A., Conde, A., & De Damborenea, J. J. (2002). Cerium: A suitable green corrosion inhibitor for tinplate. *Corrosion Science*, *44*(3), 511–520. Available from https://doi.org/10.1016/s0010-938x(01)00053-1.

Behzadnasab, M., Mirabedini, S. M., Kabiri, K., & Jamali, S. (2011). Corrosion performance of epoxy coatings containing silane treated ZrO_2 nanoparticles on mild steel in 3.5% NaCl solution. *Corrosion Science*, *53*(1), 89–98. Available from https://doi.org/10.1016/j.corsci.2010.09.026.

Bentiss, F., Traisnel, M., & Lagrenee, M. (2000). The substituted 1,3,4-oxadiazoles: a new class of corrosion inhibitors of mild steel in acidic media. *Corrosion Science*, *42*(1), 127–146. Available from https://doi.org/10.1016/S0010-938X(99)00049-9.

Brusic, V., Frisch, M. A., Eldridge, B. N., Novak, F. P., Kaufman, F. B., Rush, B. M., & Frankel, G. S. (1991). Copper corrosion with and without inhibitors. *Journal of the Electrochemical Society*, *138*(8), 2253–2259. Available from https://doi.org/10.1149/1.2085957.

Chetouani, A., & Hammouti, B. (2003). Corrosion inhibition of iron in hydrochloric acid solutions by naturally henna. *Bulletin of Electrochemistry*, *19*, 23–25.

Cudennec, Y., & Lecerf, A. (2003). The transformation of $Cu(OH)_2$ into CuO, revisited. *Solid State Sciences*, *5*(11–12), 1471–1474. Available from https://doi.org/10.1016/j.solidstatesciences.2003.09.009.

Deepa, K., & Nayaka, Y. A. (2020). Synthesis of CuO micro and nanoparticles as composite additives for corrosion resistant Zn-composite coatings on mild steel. *Inorganic and Nano-Metal Chemistry*, *50*(5), 354–360. Available from https://doi.org/10.1080/24701556.2019.1711404.

Dhineshbabu, N. R., Rajendran, V., Nithyavathy, N., & Vetumperumal, R. (2016). Study of structural and optical properties of cupric oxide nanoparticles. *Applied Nanoscience (Switzerland)*, *6*(6), 933–939. Available from https://doi.org/10.1007/s13204-015-0499-2.

Fan, G., & Li, F. (2011). Effect of sodium borohydride on growth process of controlled flower-like nanostructured Cu_2O/CuO films and their hydrophobic property. *Chemical Engineering Journal*, *167*(1), 388–396. Available from https://doi.org/10.1016/j.cej.2010.12.090.

Fiala, A., Boukhedena, W., Lemallem, S. E., Brahim Ladouani, H., & Allal, H. (2019). Inhibition of carbon steel corrosion in HCl and H_2SO_4 Solutions by ethyl 2-Cyano-2-(1,3-dithian-2-ylidene) acetate. *Journal of Bio- and Tribo-Corrosion*, *5*(2), 42. Available from https://doi.org/10.1007/s40735-019-0237-5.

Francesco, R., Giorgio, S., Giovanni, M., Emma, A., & Giancarlo, L. (2011). EIS study on the corrosion performance of a Cr(III)-based conversion coating on zinc galvanized steel for the automotive industry. *Journal of Solid State Electrochemistry*, *15*, 703–709. Available from https://doi.org/10.1007/s10008-010-1140-7.

Gao, S., Yang, S., Shu, J., Zhang, S., Li, Z., & Jiang, K. (2008). Green fabrication of hierarchical CuO hollow micro/nanostructures and enhanced performance as electrode materials for lithium-ion batteries. *Journal of Physical Chemistry C*, *112*(49), 19324–19328. Available from https://doi.org/10.1021/jp808545r.

Gong, Z., Wang, J., Wu, L., Wang, X., Lü, G., & Liao, L. (2013). Fabrication of super hydrophobic surfaces on copper by solution-immersion. *Chinese Journal of Chemical Engineering*, *21*(8), 920–926. Available from https://doi.org/10.1016/S1004-9541(13)60569-8.

Huang, J., Liu, Y., Yuan, J., & Li, H. (2014). Al/Al_2O_3 composite coating deposited by flame spraying for marine applications: Alumina skeleton enhances anti-corrosion and wear performances. *Journal of Thermal Spray Technology*, *23*(4), 676–683. Available from https://doi.org/10.1007/s11666-014-0056-7.

Karpakam, V., Kamaraj, K., Sathiyanarayanan, S., Venkatachari, G., & Ramu, S. (2011). Electrosynthesis of polyaniline-molybdate coating on steel and its corrosion protection performance. *Electrochimica Acta*, *56*(5), 2165–2173. Available from https://doi.org/10.1016/j.electacta.2010.11.099.

Kumar, H., Rajrani, R., Yadav, A., & Rajni. (2020). Synthesis, characterization and influence of reduced Graphene Oxide (rGO) on the performance of mixed metal oxide nano-composite as optoelectronic material and corrosion inhibitor. *Chemical Data Collections: The Newsletter of the Archives and Special Collections on Women in Medicine, the Medical College of Pennsylvania*, *29*100527. Available from https://doi.org/10.1016/j.cdc.2020.100527.

Lekka, M., Koumoulis, D., Kouloumbi, N., & Bonora, P. L. (2009). Mechanical and anticorrosive properties of copper matrix micro- and nano-composite coatings. *Electrochimica Acta*, *54*(9), 2540–2546. Available from https://doi.org/10.1016/j.electacta.2008.04.060.

Liu, J., Huang, X., Li, Y., Li, Z., Chi, Q., & Li, G. (2008). Formation of hierarchical CuO microcabbages as stable bionic superhydrophobic materials via a room-temperature solution-immersion process. *Solid State Sciences*, *10*(11), 1568–1576. Available from https://doi.org/10.1016/j.solidstatesciences.2008.02.005.

Ma, H., Chen, S., Yin, B., Zhao, S., & Liu, X. (2003). Impedance spectrospic study of corrosion inhibition of copper by surfactants in the acidic solutions. *Corrosion Science*, *45*(5), 867–882. Available from https://doi.org/10.1016/S0010-938X(02)00175-0.

Martini, E. M. A., & Muller, I. L. (2000). Characterization of the film formed on iron borate solution by electrochemical impedance spectroscopy. *Corrosion Science*, *42*(3), 443–454. Available from https://doi.org/10.1016/S0010-938X(99)00064-5.

Metikoš-Huković, M., Babić, R., & Marinović, A. (1998). Spectrochemical characterization of benzotriazole on copper. *Journal of the Electrochemical Society*, 4045–4051. Available from https://doi.org/10.1149/1.1838912.

Mohammad, B., Mahamood, A., & Mehdi, A. (2017). $CuZnAl_2O_3$ nanocomposites: Study of microstructure, corrosion, and wear properties. *International Journal of Minerals, Metallurgy and Materials*, *24*, 462–472. Available from https://doi.org/10.1007/s12613-017-1427-0.

Popova, A., Sokolova, E., Raicheva, S., & Christov, M. (2003). AC and DC study of the temperature effect on mild steel corrosion in acid media in the presence of benzimidazole derivatives. *Corrosion Science*, *45*(1), 33–58. Available from https://doi.org/10.1016/S0010-938X(02)00072-0.

Raja, P. B., Ismail, M., Ghoreishiamiri, S., Mirza, J., Ismail, M. C., Kakooei, S., & Rahim, A. A. (2016). Reviews on corrosion inhibitors: A short view. *Chemical Engineering Communications*, *203*(9), 1145–1156. Available from https://doi.org/10.1080/00986445.2016.1172485.

Ruhi, G., Bhandari, H., & Dhawan, S. K. (2014). Designing of corrosion resistant epoxy coatings embedded with polypyrrole/SiO_2 composite. *Progress in Organic Coatings*, *77*(9), 1484–1498. Available from https://doi.org/10.1016/j.porgcoat.2014.04.013.

Selvaraj, P. K., Sivakumar, S., & Selvaraj, S. (2019). Embargo nature of CuO-PANI composite against corrosion of mild steel in low pH medium. *Journal of Electrochemical Science and Technology*, *10*(2), 139–147. Available from https://doi.org/10.5229/JECST.2019.10.2.139.

Sengupta, S., Murmu, M., Mandal, S., Hirani, H., & Banerjee, P. (2021). Competitive corrosion inhibition performance of alkyl/acyl substituted 2-(2-hydroxybenzylideneamino)phenol protecting mild steel used in adverse acidic medium: A dual approach analysis using FMOs/molecular dynamics simulation corroborated experimental findings. *Colloids and Surfaces A: Physicochemical and Engineering Aspects*, *617*126314. Available from https://doi.org/10.1016/j.colsurfa.2021.126314.

Sengupta, S., Murmu, M., Murmu, N. C., & Banerjee, P. (2021). Adsorption of redox-active Schiff bases and corrosion inhibiting property for mild steel in 1 mol L^{-1} H_2SO_4: Experimental analysis supported by ab initio DFT, DFTB and molecular dynamics simulation approach. *Journal of Molecular Liquids*, *326*115215. Available from https://doi.org/10.1016/j.molliq.2020.115215.

Shaterian, M., Khoobi, A., Enhessari, M., & Ozaee, K. (2015). A new strategy based on thermodiffusion of ceramic nanopigments into metal surfaces and formation of anti-corrosion coatings. *Microporous and Mesoporous Materials*, *218*, 62–68. Available from https://doi.org/10.1016/j.micromeso.2015.06.039.

She, Z., Li, Q., Wang, Z., Li, L., Chen, F., & Zhou, J. (2012). Novel method for controllable fabrication of a superhydrophobic CuO surface on AZ91D magnesium alloy. *ACS Applied Materials and Interfaces*, *4*(8), 4348–4356. Available from https://doi.org/10.1021/am3009949.

Singh, D. P., Ojha, A. K., & Srivastava, O. N. (2009). Synthesis of different $Cu(OH)_2$ and CuO (nanowires, rectangles, seed-, belt-, and sheetlike) nanostructures by simple wet chemical route. *Journal of Physical Chemistry C*, *113*(9), 3409–3418. Available from https://doi.org/10.1021/jp804832g.

Solmaz, R., Altunbaş Şahin, E., & Kardaş, G. (2011). Electrochemical preparation and characterization of nickel and zinc-modified poly-2-aminothiazole films on mild steel surface and their corrosion inhibition performance. *Reactive and Functional Polymers*, *71*(12), 1148–1154. Available from https://doi.org/10.1016/j.reactfunctpolym.2011.09.002.

Soufeiani, L., Foliente, G., Nguyen, K. T. Q., & San Nicolas, R. (2020). Corrosion protection of steel elements in façade systems—A review. *Journal of Building Engineering*, *32*, 101759. Available from https://doi.org/10.1016/j.jobe.2020.101759.

Stipaničev, M., Turcu, F., Esnault, L., Schweitzer, E. W., Kilian, R., & Basseguy, R. (2013). Corrosion behavior of carbon steel in presence of sulfate-reducing bacteria in seawater environment. *Electrochimica Acta*, *113*, 390–406. Available from https://doi.org/10.1016/j.electacta.2013.09.059.

Strehblow, H. H., & Titze, B. (1980). The investigation of the passive behaviour of copper in weakly acid and alkaline solutions and the examination of the passive film by esca and ISS. *Electrochimica Acta*, *25*(6), 839–850. Available from https://doi.org/10.1016/0013-4686(80)90036-5.

Umoren, S. A., & Eduok, U. M. (2016). Application of carbohydrate polymers as corrosion inhibitors for metal substrates in different media: A review. *Carbohydrate Polymers*, *140*, 314–341. Available from https://doi.org/10.1016/j.carbpol.2015.12.038.

Xhanari, K., & Finšgar, M. (2019). Organic corrosion inhibitors for aluminum and its alloys in chloride and alkaline solutions: A review. *Arabian Journal of Chemistry*, *12*(8), 4646–4663. Available from https://doi.org/10.1016/j.arabjc.2016.08.009.

Xiao, F., Yuan, S., Liang, B., Li, G., Pehkonen, S. O., & Zhang, T. (2015). Superhydrophobic CuO nanoneedle-covered copper surfaces for anticorrosion. *Journal of Materials Chemistry A*, *3*(8), 4374–4388. Available from https://doi.org/10.1039/c4ta05730a.

Yao, W., Liang, W., Huang, G., Jiang, B., Atrens, A., & Pan, F. (2020). Superhydrophobic coatings for corrosion protection of magnesium alloys. *Journal of Materials Science and Technology*, *52*, 100–118. Available from https://doi.org/10.1016/j.jmst.2020.02.055.

Zanella, C., Lekka, M., & Bonora, P. L. (2009). Influence of the particle size on the mechanical and electrochemical behaviour of micro- and nano-nickel matrix composite coatings. *Journal of Applied Electrochemistry*, *39*(1), 31–38. Available from https://doi.org/10.1007/s10800-008-9635-y.

Zhang, W., Li, H.-J., Wang, M., Wang, L.-J., Zhang, A.-H., & Wu, Y.-C. (2019). Highly effective inhibition of mild steel corrosion in HCl solution by using pyrido[1,2-a]benzimidazoles. *New Journal of Chemistry*, *43*(1), 413–426. Available from https://doi.org/10.1039/C8NJ04028A.

Zhu, K., Li, X., Wang, H., Li, J., & Fei, G. (2017). Electrochemical and anti-corrosion behaviors of water dispersible graphene/acrylic modified alkyd resin latex composites coated carbon steel. *Journal of Applied Polymer Science*, *134*(11). Available from https://doi.org/10.1002/app.44445.